Electron and Electromagnetic Field Dynamics in Nanostructures

Department of Theoretical and Computational Molecular Science
Division of Theoretical Molecular Science I

NOBUSADA, Katsuyuki	Associate Professor
YASUIKE, Tomokazu	Assistant Professor
IWASA, Takeshi	JSPS Post-Doctral Fellow
KUBOTA, Yoji	Post-Doctoral Fellow
NODA, Masashi	Post-Doctoral Fellow
YAMADA, Mariko	Secretary

We have developed theoretical methods to calculate photo-induced electron dynamics in nanostructured materials such as nanoparticles, quantum-dot arrays, and adsorbate-surface systems. Specifically, we have developed generalized theory of a light-matter interaction beyond a dipole approximation on the basis of the multipolar Hamiltonian with the aim of understanding the near-field excitation of molecules at the 1 nm scale. Optical forces exerted on a 1 nm-sized metal particle were calculated in the framework of real-time and real-space time-dependent density functional theory combined with the new light-matter interaction formalism. We have also studied exciton–polariton transmission in quantum dot waveguides in an array of quantum dot. Furthermore, collectivity of plasmonic excitations in small sodium clusters was investigated in depth.

1. Near-Field Induced Optical Force on a Metal Particle and C_{60}: Real Time and Real Space Electron Dynamics Simulation$^{1)}$

Optical forces induced by a near-field are calculated for a 1 nm-sized metal particle mimicked by a jellium model and for C_{60} in the framework of real-time and real-space time-dependent density functional theory combined with a non-uniform light-matter interaction formalism, fully taking account of multipole interaction. A highly localized near-field non-uniformly polarizes these molecules. The locally induced polarization charges in the molecules are partly canceled by the screening charges. The polarization and screening charges generally contribute to the attractive and repulsive forces, respectively, and a sensible balance between these charges results in several peaks in the optical force as a function of the frequency of the near-field. The resonance excitation does not necessarily maximally induce the net force and the force exerted on the molecules strongly depends on the details of their electronic structures. The optical force is larger in the metal particle than C_{60}. We also found that the optical force depends linearly on the intensity of the near-field.

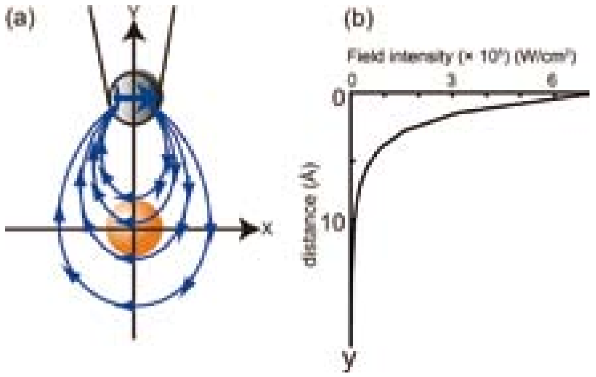

Figure 1. (a) Schematic of a near-field fiber tip (gray ball) and a target particle (orange ball). The near-field is approximated by the radiation from an *x*-polarized oscillating dipole (solid blue arrow). The blue curves denote the electric field lines. (b) Electric field intensity as a function of distance between the tip and the particle.

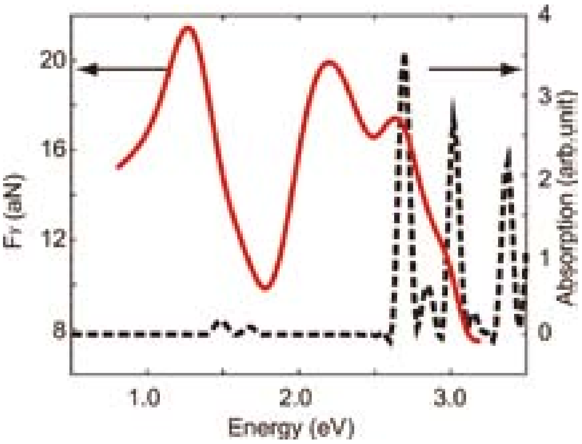

Figure 2. Absorption spectrum (dashed-black) of the silver nanoparticle and the time-averaged force on the particle (red) as a function of energy.

2. Exciton–Polariton Transmission in Quantum Dot Waveguides and a New Transmission Path due to Thermal Relaxation[2)]

Exciton–polariton transmission in quantum dot waveguides is investigated with quantum time-evolution equations in Liouville space for exciton wave packet dynamics. The transmission efficiency of the exciton–polariton wave with the longitudinal and transverse mode transformation strongly depends on the geometric parameters (bending angle and interdot distance) of the waveguides and on configuration of an additional branch attached to the waveguide. We have numerically demonstrated the transmission efficiency significantly improves by controlling these geometric parameters and the configuration of the branched waveguide. The optimal bending angle for efficient transmission with the longitudinal and transverse mode transformation deviates from the right angle owing to more than nearest-neighbor-site interactions through a shortcut. We have also found that existence of thermal relaxation enables to open a new transmission channel along which the exciton–polariton transmission through the Coulomb interaction is suppressed.

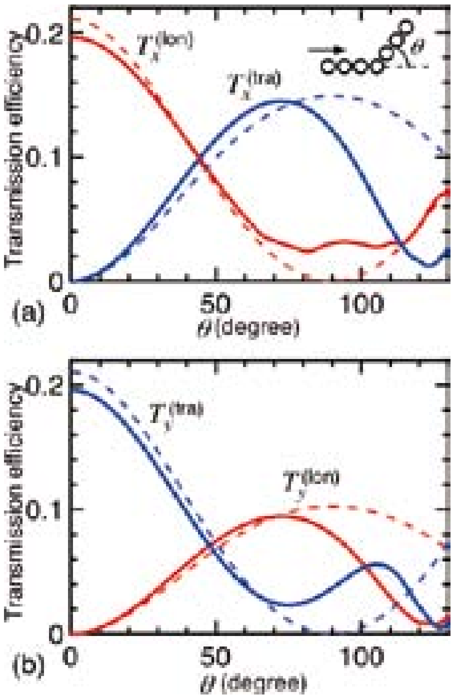

Figure 3. Bending angle dependence of transmission efficiency. The solid and dashed curves are the results for the full interaction calculations and for the calculation under the nearest-neighbor interaction approximation, respectively.

3. Collectivity of Plasmonic Excitations in Small Sodium Clusters

Plasmonic excitations in small sodium clusters are investigated by using the linear-response density functional theory (LRDFT). The computed photoabsorption spectra show a small number of strong peaks, and the intensities for some of those peaks monotonically grow up with increasing the cluster size. The dipolar character of the transition density distributions for them shows a clear correspondence to a classical picture of plasmonic excitation. The collectivity of the electronic motion induced by the plasmonic excitation is quantitatively analyzed in terms of the collectivity index defined by the transition density matrix. The excitation mode dependence of the collectivity in non-spherical clusters and large collectivities for the higher-energy plasmonic excitations are found. The collectivity analysis also clarifies the existence of the non-dipolar collective motion at the energies very close to the higher-energy plasmonic excitations. The importance of the non-dipolar motion is pointed out in light of nano-optics.

4. Isolation, Structure, and Stability of a Dodecanethiolate-Protected $\mathrm{Pd_1Au_{24}}$ Cluster[3)]

A dodecanethiolate-protected $\mathrm{Pd_1Au_{24}(SC_{12}H_{25})_{18}}$ cluster, which is a mono-Pd-doped cluster of the well understood magic gold cluster $\mathrm{Au_{25}(SR)_{18}}$, was isolated in high purity using solvent fractionation and high-performance liquid chromatography (HPLC) after the preparation of dodecanethiolate-protected palladium–gold bimetal clusters. The cluster thus isolated was identified as the neutral $[\mathrm{Pd_1Au_{24}(SC_{12}H_{25})_{18}}]^0$ from the retention time in reverse phase columns and by elemental analyses. The LDI mass spectrum of $[\mathrm{Pd_1Au_{24}(SC_{12}H_{25})_{18}}]^0$ indicates that $[\mathrm{Pd_1Au_{24}(SC_{12}H_{25})_{18}}]^0$ adopts a similar framework structure to $\mathrm{Au_{25}(SR)_{18}}$, in which an icosahedral Au^{13} core is protected by six [–S–Au–S–Au–S–] oligomers. The optical absorption spectrum of $[\mathrm{Pd_1Au_{24}(SC_{12}H_{25})_{18}}]^0$ exhibits peaks at ~690 and ~620 nm, which is consistent with calculated results on $[\mathrm{Pd_1@Au_{24}(SC_1H_3)_{18}}]^0$ in which the central gold atom of $\mathrm{Au_{25}(SC_1H_3)_{18}}$ is replaced with Pd. These results strongly indicate that the isolated $[\mathrm{Pd_1Au_{24}(SC_{12}H_{25})_{18}}]^0$ has a core-shell $[\mathrm{Pd_1@Au_{24}(SC_{12}H_{25})_{18}}]^0$ structure in which the central Pd atom is surrounded by a frame of $\mathrm{Au_{24}(SC_{12}H_{25})_{18}}$. Experiments on the stability of the cluster showed that $\mathrm{Pd_1@Au_{24}(SC_{12}H_{25})_{18}}$ is more stable against degradation in solution and laser dissociation than $\mathrm{Au_{25}(SC_{12}H_{25})_{18}}$. These results indicate that the doping of a central atom is a powerful method to increase the stability beyond the $\mathrm{Au_{25}(SR)_{18}}$ cluster.

References

1) T. Iwasa and K. Nobusada, *Phys. Rev. A* **80**, 043409 (11 pages) (2009).
2) Y. Kubota and K. Nobusada, *J. Phys. Soc. Jpn.* **78**, 114603 (7 pages) (2009).
3) Y. Negishi, W. Kurashige, Y. Niihori, T. Iwasa and K. Nobusada, *Phys. Chem. Chem. Phys.* **12**, 6219–6225 (2010).